Supplementary Materials:

Materials and Methods

Supplementary Figure Legends

Supplementary Figures S1-S9

Supplementary Tables S1-S6

Materials and Methods

Healthy volunteers

Healthy volunteers gave written informed consent with regard to scientific use (Sanquin Blood bank, Nijmegen, the Netherlands)

Reagents

Ficoll-Paque (GE Healthcare) was used to isolate PBMCs by differential centrifugation. The RPMI 1640 medium (Sigma-Aldrich) was supplemented with 10 μg/mL gentamycin, 10 mM L-glutamine and 10 mM pyruvate (Life Technologies). β1,3(D)glucan (β-glucan) was kindly provided by Prof. David Williams (University of Tennessee). Pam3Cys were purchased from EMC microcollections and LPS (E. coli serotype 055:B5) were purchased from Sigma-Aldrich, with an additional purification step (*64*). For "inhibition" experiments H89 (Sigma-Aldrich, B1427), propranolol (Sigma-Aldrich, P0884), 2',5'-dideoxyadenosine (Sigma-Aldrich, D7408), human recombinant IL10 (Merck-Millipore) were used.

Isolation of primary monocytes for genome-wide sequencing analysis

Monocytes were obtained by depletion of CD3, CD19 and CD56 positive cells from PBMCs obtained upon Ficoll isolation of a buffycoat. CD3 MicroBeads (130-050-101), CD19 MicroBeads (130-050-301) and CD56 were purchased at Miltenyi Biotec and used according to the manufacturer protocol. Efficacy of depletion was controlled by flow cytometry (Fig. S1A). Samples were measured on a FACS FC500, and data were analyzed using the CXP software (Beckman Coulter). Before and after the depletion, cells were incubated in PBS supplemented with 1% PBA and the following antibodies: anti-CD45-PeCy7 (Beckman Coulter), anti-CD14-FITC (Beckman Coulter), anti-CD3-PC5 (Biolegend (ITK)), anti-CD19-ECD (Beckman Coulter) and anti-56-PE (BD Bioscience). For the additional transcriptomic analysis of the pop-1 and pop-2 samples (Fig. S1A), additional CD14 positive cells selection was performed on the CD3-, CD19- and CD56- population using CD14 MicroBeads (130-050-201) from Miltenyi Biotec. By this selection monocytes population (Mo) was further defined into monocytes highly expressing CD14 (pop-1, ~88% of the Mo) and the rest of the Mo (pop-2, ~12% of the Mo) (Fig. S1 A, B).

For ChIP analysis and DNase I treatment, $10x10^6$ of CD3-,CD19- and CD56-depleted monocytes were plated on 100 mm dishes. Monocytes were pre-incubated either with cell culture medium (RPMI), β-glucan (5 μg/mL) or with LPS (100 ng/mL), for 24 hours in a total volume of 10 mL. After wash-out, cells were cultured in RPMI supplemented with 10% human pooled serum **containing homeostatic levels of M-CSF that induces monocyte differentiation**. Cell samples were collected at 0 hours and on 6^{th} day, and counted before further treatment for chromatin immunoprecipitation or DNase I treatment.

For RNASeq $5x10^6$ of CD3-CD19-CD56- depleted monocytes were seeded on 60 mm dishes. Monocytes were pre-incubated either with cell culture medium (RPMI), β-glucan (5 μg/mL) or with LPS (100 ng/mL) for 24 hours. After wash-out, cells were cultured in RPMI supplemented with 10% human pool serum and further RNA collection and library preparation (0 hours and 5 days after treatment) was done according to standard BLUEPRINT protocols (www.blueprint-epigenome.eu) and Illumina library preparation protocol.

For cytokines production, $1x10^4$ of CD3-CD19-CD56- depleted monocytes were plated out in a 96 well flat bottom plate. Monocytes were pre-incubated as above for 24 hours in a total volume of 200 μL. After a wash-out, cells were cultured in RPMI supplemented with 10% human pooled serum. Cells were then subjected after 5 days to a second stimulation for 24 hours with (LPS 10 ng/mL) or P3C (10 μg/mL) for cytokine measurements with ELISA (Fig. S4E). Each volunteer used in this assay presented an efficient training or tolerant phenotype (data not shown).

Inhibition experiments

PBMCs were diluted to a concentration of $5x10^6$ cells per mL and 100 μL of this suspension was added to the well of a 96-well plate. PBMCs were incubated for 1 hour at 37°C in 5% CO2 and adherent monocytes were selected by washing out non-adherent cells with pre-warmed PBS. For training, monocytes were pre-incubated with β-glucan (5 μg/mL) for 24 hours. For tolerance, cells were pre-incubated with LPS (100 ng/mL) for 24 hours. Cells were then washed and maintained in RPMI supplemented with 10% human pool serum. For cytokine measurements cells were subjected to a second stimulation of cytokine production after a period of 6 days with various stimuli in a volume of 200 μl of medium (LPS 10 ng/mL, Pam3Cys 10

μg/mL). After 24 hours, supernatants were collected and stored at -20°C until assayed.

In the "inhibition of training" experiments, before the priming with β-glucan, adherent monocytes were pre-incubated for 1 hour with H89 (30 μM), 2',5'-dideoxyadenosine (1 mM) or propranolol (200 μM).

Cytokine assays

TNFα, IL-6, Il-1β and IL10 were measured using ELISA according to the manufacturer protocol (IL6, IL10: Sanquin; and TNFα, IL1β: R&D). For cytokines production assays and qPCR analysis, the differences between groups were analyzed using the Wilcoxon signed-rank test (unless otherwise stated). The level of significance was defined as a p-value < 0.05.

Western-blot

Immunoblotting experiments were performed as previously described (*17*). The quantification of protein expression was performed by densitometry (GS-670, Bio-Rad, Hercules, CA) and signal analysis using Molecular Analyst software (Bio-Rad). The ratio between the intensity of the protein of interest and β-actin was calculated. The activation of caspase-1 was assessed by calculating the ratio between the p10 and p45 fragments.

RNA-seq alignment and expression analysis

RNA-seq reads were aligned using GSNAP (*65*) using non-default parameters -m 1 -N 1 -n 1 -Q -s Ensembl_splice_68. RNA-seq library data were initially subjected to a quality control step, where, based on read distribution over the annotated genome, libraries that are outliers were identified and discarded from further analysis. For expression analyses reads were aligned to the Ensembl v68 human transcriptome using Bowtie. Quantification of gene expression was performed using MMSEQ (*31*).

Differential expression

Differential expression was determined using MMDIFF (*32*). A two model comparison was used to identify differentially expressed genes that confer cellular identity Mo/Mf. Under the null-model the mean expression level is the same in both cell types and under the alternative model the mean expression level is allowed to

differ between the two cell types. Genes with a larger posterior probability for the second model, an RPKM value greater than 2 in any of Mo or Mf and minimally a two-fold expression change were considered as differentially expressed.

Expression changes related to LPS and β-glucan were studied using a 15-model comparison, a.k.a. polytomous comparison. Under the null-model, it is assumed that the mean expression level is the same across differentiation and micro-organismal ligand response. In the most complex model the mean expression level is assumed to be different for all conditions (Mo, Mf, LPS-Mf, BG-Mf). Additionally, we defined 4 models that assume a mean expression in one condition that differs from the equal expression in the three others, 3 models that assume two pairs of conditions with equal mean expression within a pair but different between the two pairs and, 6 models that assume the remaining possibility that two conditions have equal mean expression while the two others have different mean expression levels that also differ from each other. We calculated the Bayes factor for each model by comparing the differential expression models to the (reference) null-model and applied Bayes' theorem to compute the posterior probability of each model per gene. The expression change directionality of a gene was determined based on the model with the highest posterior probability having to be at least 0.35 for the gene to be considered for downstream analyses.

Condensing genes into six expression modules

Genes that were successfully assigned to expression models that assume differential expression in monocyte-derived macrophages were grouped based on their expression in LPS-Mf and BG-Mf relative to Mf. We applied a three group classification (up, down and equal) to record the direction of expression change in LPS-Mf and BG-Mf relative to Mf, resulting in eight possible expression scenarios. Scenarios "LPS-Mf is down, BG-Mf is up" and "LPS-Mf is up, BG-Mf is down" were dropped because of low (3 and 5 respectively) gene numbers. The six remaining scenarios were relabeled as expression modules: M1="LPS-Mf is down, BG-Mf is down", M2=LPS-Mf is down, BG-Mf is equal", M3="LPS-Mf is equal, BG-Mf is down", M4=" LPS-Mf is equal, BG-Mf is up", M5="LPS-Mf is up, BG-Mf is equal", M6="LPS-Mf is up, BG-Mf is up.

ChIP-seq

H3K4me1, H3K4me3 and H3K27ac antibodies were extensively characterized (see www.blueprint-epigenome.eu) and used for ChIP according to standard BLUEPRINT protocols (www.blueprint-epigenome.eu).

Peak Calling and identification of differential regulatory regions

For peak calling the BAM files were first filtered to remove the reads with mapping quality less than 15, followed by fragment size modeling (http://code.google.com/p/phantompeakqual-tools/). The peak calling algorithm MACS2 (http://github.com/taoliu/MACS/) was used to detect the binding sites for the three studied histone marks at p-value of 10-10. H3K4me1 peaks were called using the broad setting of MACS2 while H3K27ac and H3K4me3 were called using the default (narrow) setting.

In order to identify differential H3K27ac-bound regulatory elements, initially, H3K27ac peaks from different treatments were merged and sequenced reads were counted from normalized data files (down scaling). H3K27ac peaks that do not overlap with H3K4me3 marked promoters (transcription start site±2.5kb) were regarded as distal regulatory elements (ACe's) whereas those overlapping with H3K4me3 marked promoters were labeled as active promoters (ACp's, Table S3). H3K27ac regions that show a change of mean ± 2x median absolute deviation (p-vlaue < 0.05) acetylation signal in each data set were regarded as dynamic acetylated regions. K-means clustering (Pearson correlation) was performed to identify different clusters dynamic H3K27ac regions (ACe1-5 and ACp1-3). The same approach was used to identify dynamic clusters of H3K4me1 (MM) or H3K4me3 (TM) marked regions that lack H3K27ac (Fig. S2).

Principal Component Analysis

We performed principal component analysis (PCA) using prcomp function in R to visualize differences between the cell types and examine reproducibility between samples of the same cell type. Treating each histone modification separately, we computed combinations of enrichment levels that capture a large proportion of the variation between cell types (PC1 and PC2). This revealed that at the single histone modification level monocytes and macrophages are distinguishable and cluster by pattern similarity of a given cell type, suggesting a high degree of reproducibility between the samples.

DNase I-seq

DNase I libraries were prepared for monocytes (Mo) and all three types of differentiated macrophages (Mf, LPS-Mf and BG-Mf) as described (*66*). In brief nuclei were isolated using Buffer A (15 mM NaCl, 60 mM KCl, 1 mM EDTA, pH 8.0, 0.5 mM EGTA, pH 8.0, 15 mM Tris-HCl, pH 8.0, 0.5 mM Spermidine) supplemented with 0.015 % IGEPAL CA-630 detergent. DNase I treatment was done for 3 minutes and the reaction was stopped with stop buffer (50 mM Tris-HCl, pH 8, 100 mM NaCl, 0.10 % SDS, 100 mM EDTA, pH 8.0, 1 mM Spermidine, 0.3 mM Spermine). The sample was further fractionated on 9% Sucrose gradient for 24 hours at 25000 rpm at 16 ºC. Fractions containing fragments smaller than 1kb were purified and processed according to the Illumina library preparation protocol.

Hotspots analysis

DNase I hotspots (DHS) were scanned for the presence of TF-motifs, where a TF-motif weight matrix was available. DHS of this study Mo, Mf, LPS-Mf and BG-Mf (four donors merged) were collapsed and merged into a single set of DHS regions, which were subsequently scanned for TF-motif occurrence. A non-redundant collection of TF-motifs was generated from TF-motif repositories JASPAR, UniPROBE, Jolma/Taipale and ht-SELEX (http://dx.doi.org/10.6084/m9.figshare.819997). Out of a collection of 1406 motifs (*48*), 544 motifs for which the assigned TF is expressed (>2 RPKM) in monocytes or monocyte-derived macrophages, were obtained. The merged set of DHS regions were scanned for TF-motif presence using Gimme motifs (*48*) with dynamic TF-motif scoring cut-offs targeting a false discovery rate (FDR) of 0.01. To look at the motif enrichments in each epigenetic cluster DHS were assigned to epigenomic clusters ACe1-5 by intersection. Motif occurrences were acquired by intersection of the assigned DHSs with the motif scanning results on the merged set of DHS. Enrichment of motifs in each of the ACe's was defined by applying a hypergeometric test using the motif frequency in all distal (non-dynamic) H3K27ac regions as the background. This results in TFs that putatively regulate the activity of the distal regulatory regions. Subsequently, hierarchical clustering was performed (Euclidian distance) using the motif occurrence frequencies in the ACe cluster. TF motifs that satisfy an arbitrary

cutoff of > 5% motif presence in at least one ACe cluster were used to generate the heat map (Fig. 4D).

Animals

C57BL/6J female mice between 8 and 12 weeks of age were used (Jackson Laboratories). Experiments were approved by the Ethics Committee on Animal Experiments of the University of Athens. Mice were injected with a sublethal dose of *C. albicans* yeast (2×10^4 CFU/mouse) in a 100 μL volume of sterile pyrogen-free phosphate-buffered saline (PBS) or with saline alone. Seven days later, mice were infected intravenously with a lethal dose of *C. albicans* yeast (2×10^6 CFU/mouse). Animals received a daily intraperitoneal injections of either saline or propranolol (1 mg/kg) one day prior the sub-lethal dose *C. albicans* yeast up to 3 days after the lethal *Candida* injection. Survival upon the lethal infection was monitored daily. Survival curves were created using the product limit method of Kaplan and Meier. Comparison of two survival curves was performed using the Logrank test. The level of significance between groups was set at p-value < 0.05.

DNA replication analysis

EdU-incorporation was performed using the Click-iT EdU Imaging kit (Invitrogen) according to the supplied protocol. Isolated monocytes were seeded on cover slips placed in 6 well cell culture plates at density of 10^5 cells per each well. A day before the EdU assay, HeLa cells were seeded at 25% confluence into control wells containing cover slips. Both monocytes and HeLa cells were then exposed to EdU for 7 hours, followed by cell fixation, permeabilization and imaging according to the manufacturer's protocol.

Supplementary figure legends:

Fig. S1. **Representative flow cytometric analysis of CD3, CD56, CD19, and CD14 positive cells.** (**A**) Cells were gated on CD45+ populations before and after Microbead lymphocyte depletion (CD3, CD56, CD19) of PBMCs obtained from the buffy coats. This Monocytes population (Mo) was further fractionated based on CD14 positive Mo (pop-1, ~88% of the Mo) and the rest of the Mo (pop-2, ~12% of the Mo). (**B**) Transcriptome analysis of Mo, Mf, LPS-Mf and BG-Mf cells from different donors. The most differential cell surface markers are plotted for cell populations pop-1 and pop-2 along with the complete set of cell states obtained from the four donors included for the transcriptome and polytomous analyses.

Fig. S2. Dynamic H3K4me DNA regions stratified by k-means clustering. (A) H3K4me1-marked distal elements. (B) H3K4me3-marked elements. (C) Provenance of the epigenetic clusters as assigned by Blueprint ChromHMM data for primary human monocytes (http://ftp.ebi.ac.uk/pub/databases/blueprint/releases/current_release/homo_sapiens/hub/hub.txt;. For comparison, the whole-genome distribution of epigenetic states is rendered.

Fig. S3. Comparison of three epigenetic marks in monocyte and macrophage populations. PCA plots comparing positively and negatively selected monocytes and macrophages as a function of the histone marks H3K4me3, H3K4me1 and H3K27ac. Note that the plots discriminate between monocyte and macrophage as well as macrophages with different differentiation stimuli. (**A**) Tags were counted on a merged peak set (minimal two occurrences) and normalized for effective library size and peak length (**B**) The top 5000 most variable peaks were selected from the merged peak set. The PCA was performed with the prcomp function in R.

Fig. S4. Attenuation of innate immune defense pathways in resident macrophages compared to circulating monocytes. Human primary monocytes were obtained from PBMCs of healthy volunteers (Mo). Primary monocytes were maintained in cell culture medium supplemented with 10% of human serum for a week to obtain macrophages (Mf). (**A**) Secreted TNF-α, IL-6, IL-10, and IL-1β in monocytes or macrophages upon 24 hours of LPS stimulation as determined by ELISA. (**B**) Monocytes or macrophages were either stimulated with LPS alone (∅) or co-stimulated with LPS and different doses of human IL10 recombinant protein

(rIL10). IL-6 production in supernatants was determined after 24 hours by ELISA. Note the differential response at 1 ng/ml LPS. (**C**) Genome browser screen shot of the IL-1β. Note the decreased H3K27ac signal over the promoter region of IL-1β in day 6 macrophages (Mf) as compared to naive monocytes (Mo) as well as an accompanying decrease in the gene expression. (**D**) Caspase-1 activation in supernatants of unstimulated monocytes and macrophages of three independent healthy volunteers was analyzed by western blot using an antibody against the Caspase-1 p10 cleavage product (upper panel). The caspase-1 activation ratio (p45/p10) is represented in the lower panel. (**E**) Diagram showing the time line of the in vitro training and tolerance experiment. Pure human primary monocytes are pre-exposed either to culture medium, β-glucan (training) or to Lipopolysaccharide (LPS) for 24 hours (1st stimulation). After the 1st stimuli is washed out the cells are further incubated for 5 days in culture medium supplemented with 10% human pooled serum. Cells are then collected for genome-wide analysis. In parallel, a second in vitro stimulation (2nd stimulation) of cytokine production with different pattern recognition receptor (PRR) ligands is performed for an additional 24 hours.

Fig. S5. Absence of DNA replication in BG trained cells. The fluorescent nucleotide analog EdU was used to label chromosomal DNA undergoing replication. While HeLa cells efficiently incorporated EdU, *in vitro* monocyte-derived macrophages (Mf) did not and nor did the β-glucan trained (BG-Mf) cells.

Fig. S6. Potentially drugable targets that are differentially regulated in differentiating monocytes. (**A-C**) Kinases (**A**), G-coupled receptors (**B**) and histone modifying enzymes (**C**) that display at least a 4-fold difference (RPKM) between Mo, Mf, LPS-Mf and/or BG-Mf are plotted.

Fig. S7. Circadian cycle factors. The indicated GO terms were queried and associated factors were stratified in four categories; (**A**) factors whose transcript level is higher in monocytes than the derived macrophages, (**B**) those whose expression is higher in macrophages, (**C**) those whose expression is relatively constant and (D) those with low transcript levels.

Fig. S8. cAMP pathway factors. The average expression level (RPKM) of a selected group of cAMP signaling pathway factors is shown. Error bars represent the standard deviation across the four donors.

Fig. S9. The cAMP dependent protein kinase (PKA) inhibitor H89 had no effect on the LPS-triggered immune response. The PKA inhibitor H89 did not modulate

the induction of IL-6 and TNFα, assayed as the response to LPS direct stimulation of monocytes; $p>0.05$ (Wilcoxon signed rank test). Data show the cytokine production (ELISA) upon LPS stimulation in the presence (H89) or absence (∅) of the PKA inhibitor as mean ± SEM, n = 4 in 2 separate experiments. $p>0.05$.

Supplementary Tables

TableS1: List of genes that are differentially expressed during monocyte (Mo) to macrophages (Mf) differentiation (Fig. 1J).

TableS2: Extended list of gene ontology terms associated with differentially expressed genes during monocyte (Mo) to macrophage (Mf) differentiation (Fig 1J) and genes assigned to the expression modules M1-6 (Fig. 3B).

TableS3: List of genomic loci associated with each epigenomic clusters (Fig. 2A-B, Fig S2A-B).

TableS4: List of genes that fit into differential expression models and that are assigned to expression modules (Fig. 3A).

TableS5: List of the 1581 human DNA sequence-specific transcription factors used in this study (Fig. 4A).

TableS6: List of transcription factor motifs that are enriched in dynamic distal regulatory elements (ACe, Fig. 4D).

A

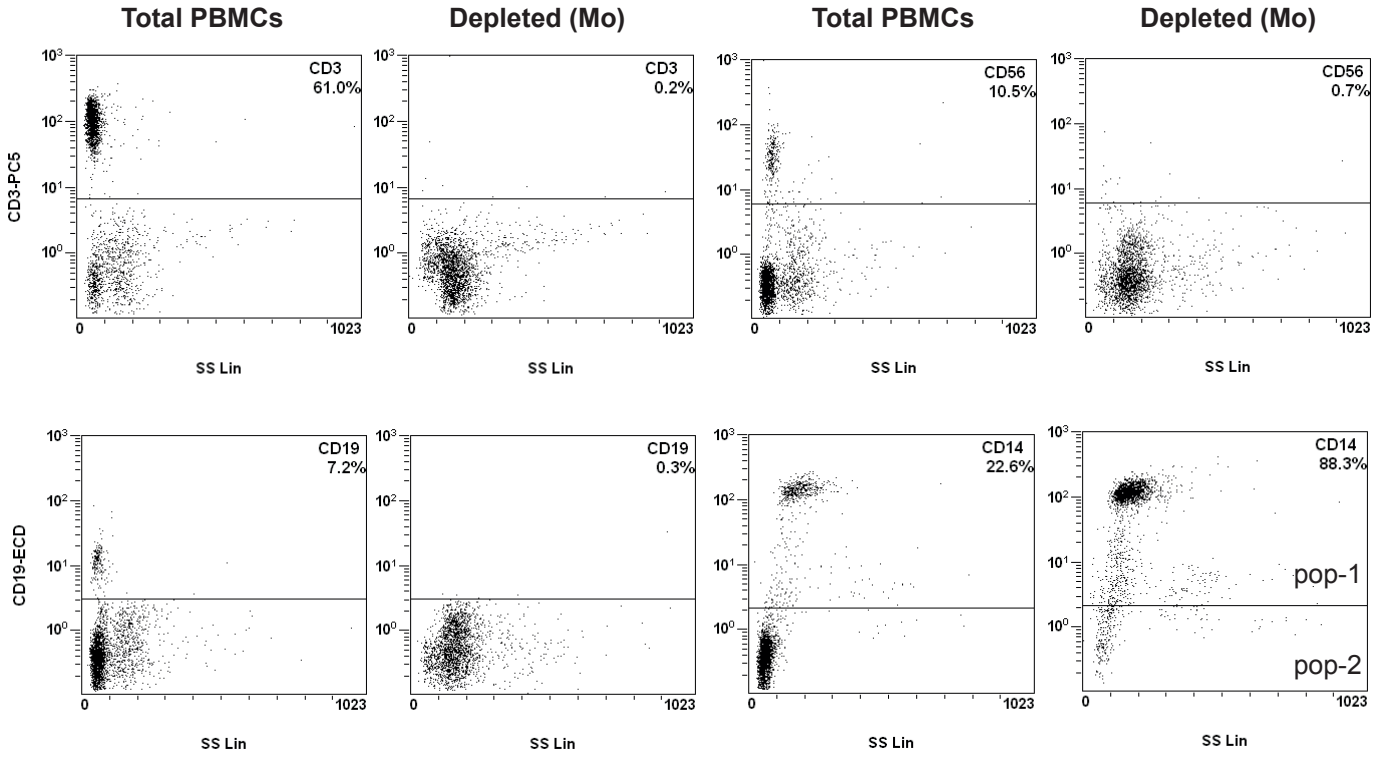
Total PBMCs
Depleted (Mo)
Total PBMCs
Depleted (Mo)
CD3-PC5
CD19-ECD
CD3
61.0%
CD3
0.2%
CD56
10.5%
CD56
0.7%
CD19
7.2%
CD19
0.3%
CD14
22.6%
CD14
88.3%
pop-1
pop-2
SS Lin

B

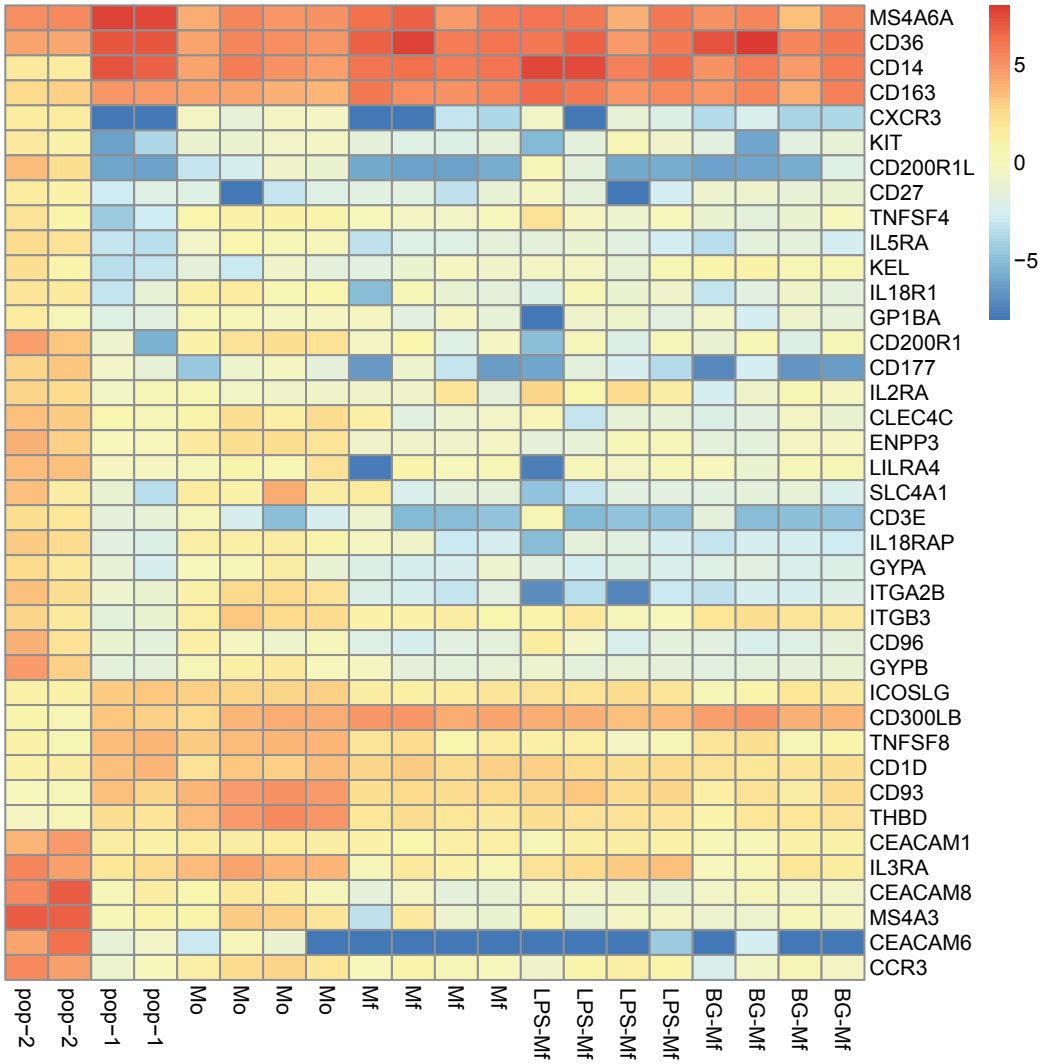
MS4A6A
CD36
CD14
CD163
CXCR3
KIT
CD200R1L
CD27
TNFSF4
IL5RA
KEL
IL18R1
GP1BA
CD200R1
CD177
IL2RA
CLEC4C
ENPP3
LILRA4
SLC4A1
CD3E
IL18RAP
GYPA
ITGA2B
ITGB3
CD96
GYPB
ICOSLG
CD300LB
TNFSF8
CD1D
CD93
THBD
CEACAM1
IL3RA
CEACAM8
MS4A3
CEACAM6
CCR3
5
0
−5
pop−2
pop−2
pop−1
pop−1
Mo
Mo
Mo
Mo
Mf
Mf
Mf
Mf
LPS-Mf
LPS-Mf
LPS-Mf
LPS-Mf
BG-Mf
BG-Mf
BG-Mf
BG-Mf

Figure S1

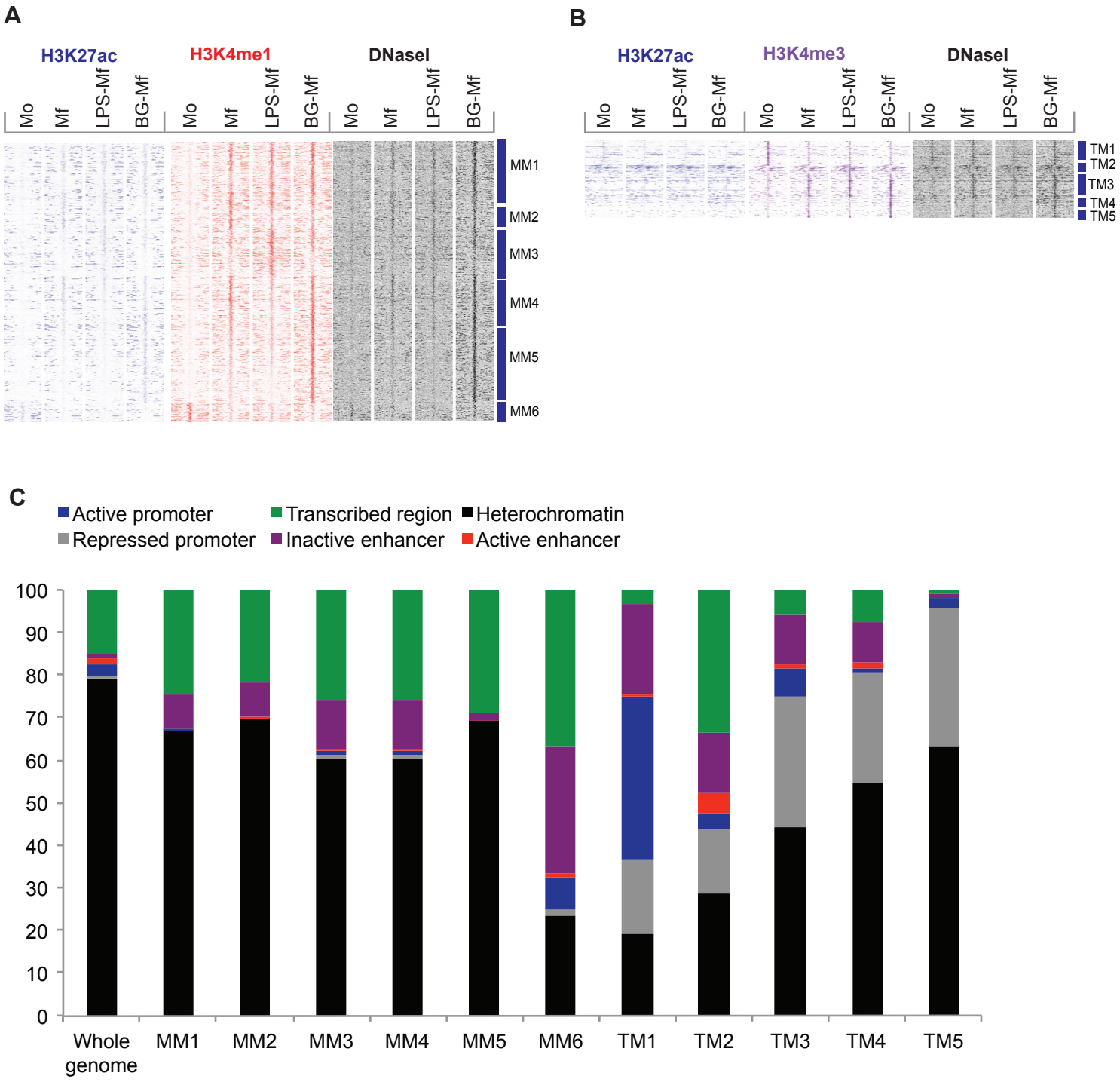
A
H3K27ac
H3K4me1
DNaseI
Mo
Mf
LPS-Mf
BG-Mf
MM1
MM2
MM3
MM4
MM5
MM6
B
H3K27ac
H3K4me3
DNaseI
TM1
TM2
TM3
TM4
TM5
C
Active promoter
Transcribed region
Heterochromatin
Repressed promoter
Inactive enhancer
Active enhancer
100
90
80
70
60
50
40
30
20
10
0
Whole genome
MM1
MM2
MM3
MM4
MM5
MM6
TM1
TM2
TM3
TM4
TM5

Figure S2

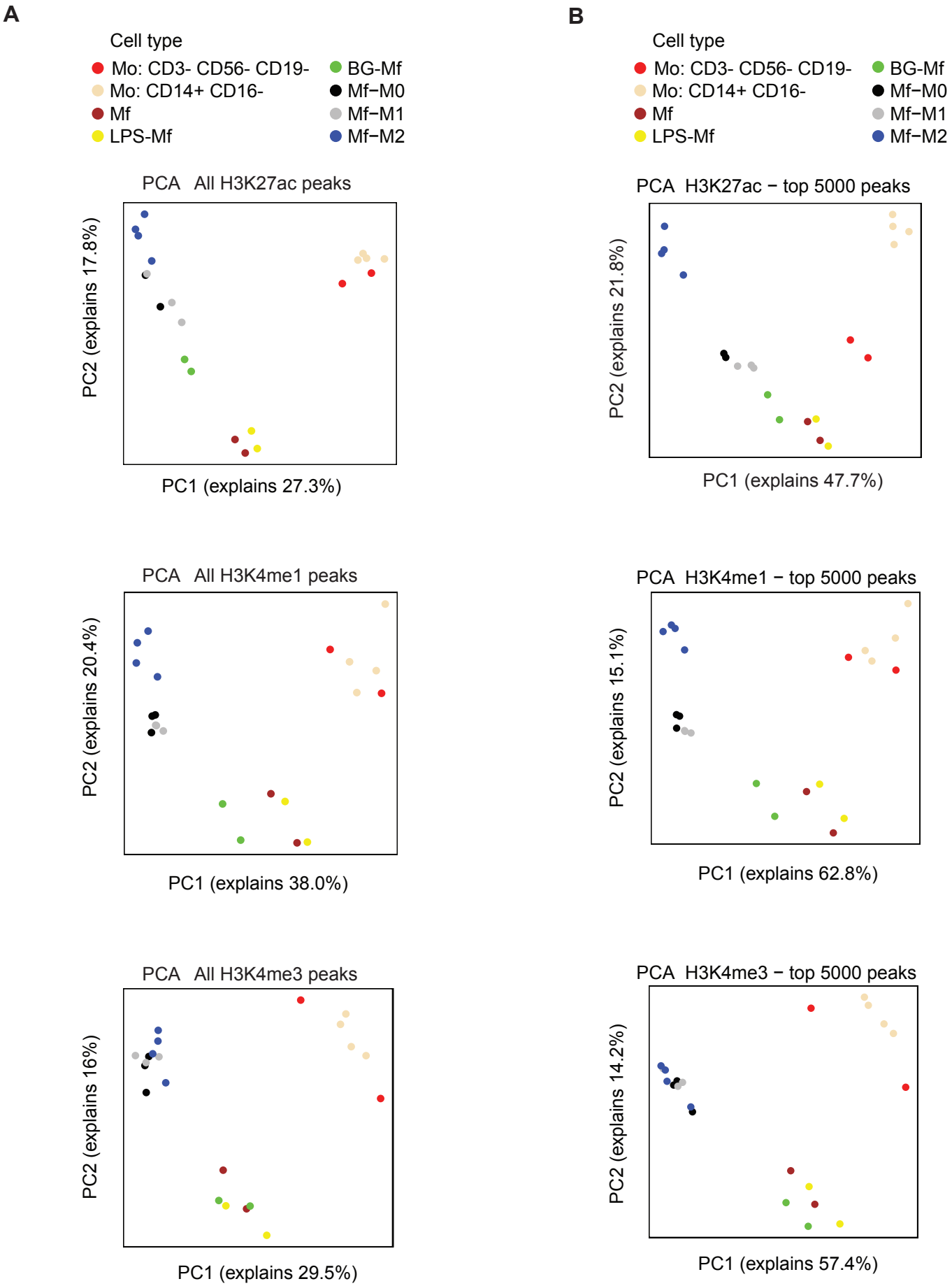
A
B
Cell type
Mo: CD3- CD56- CD19-
Mo: CD14+ CD16-
Mf
LPS-Mf
BG-Mf
Mf−M0
Mf−M1
Mf−M2
PCA All H3K27ac peaks
PC2 (explains 17.8%)
PC1 (explains 27.3%)
PCA H3K27ac − top 5000 peaks
PC2 (explains 21.8%)
PC1 (explains 47.7%)
PCA All H3K4me1 peaks
PC2 (explains 20.4%)
PC1 (explains 38.0%)
PCA H3K4me1 − top 5000 peaks
PC2 (explains 15.1%)
PC1 (explains 62.8%)
PCA All H3K4me3 peaks
PC2 (explains 16%)
PC1 (explains 29.5%)
PCA H3K4me3 − top 5000 peaks
PC2 (explains 14.2%)
PC1 (explains 57.4%)

Figure S3

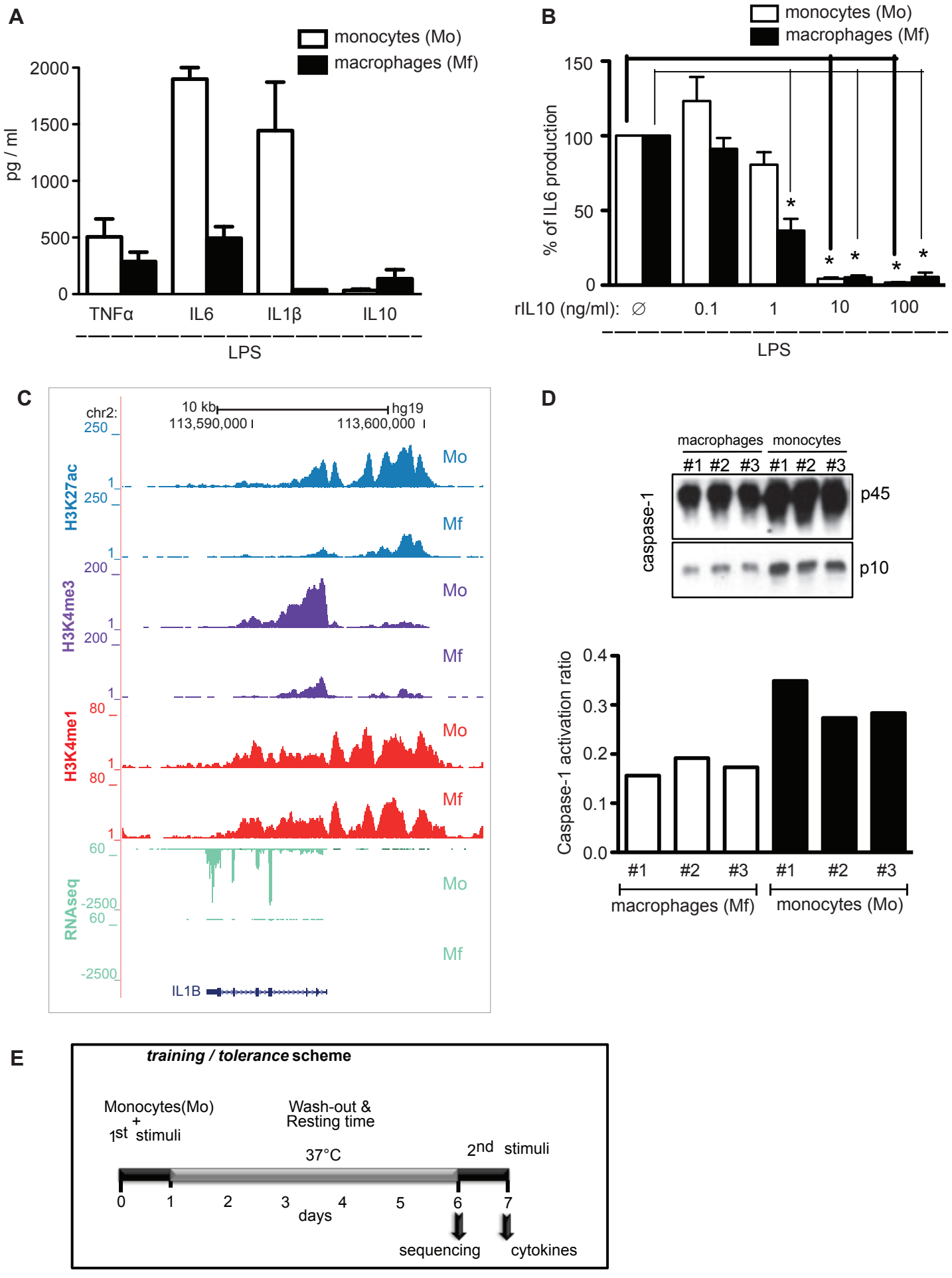
A
monocytes (Mo)
macrophages (Mf)
pg / ml
2000
1500
1000
500
0
TNFα
IL6
IL1β
IL10
LPS
B
monocytes (Mo)
macrophages (Mf)
% of IL6 production
150
100
50
0
rIL10 (ng/ml): ∅
0.1
1
10
100
LPS
C
chr2:
10 kb
hg19
113,590,000
113,600,000
H3K27ac
H3K4me3
H3K4me1
RNAseq
Mo
Mf
IL1B
D
macrophages
monocytes
#1 #2 #3 #1 #2 #3
caspase-1
p45
p10
Caspase-1 activation ratio
0.4
0.3
0.2
0.1
0.0
#1 #2 #3 #1 #2 #3
macrophages (Mf)
monocytes (Mo)
E
training / tolerance scheme
Monocytes(Mo)
+
1st stimuli
Wash-out &
Resting time
37°C
2nd stimuli
0 1 2 3 4 5 6 7
days
sequencing
cytokines

Figure S4

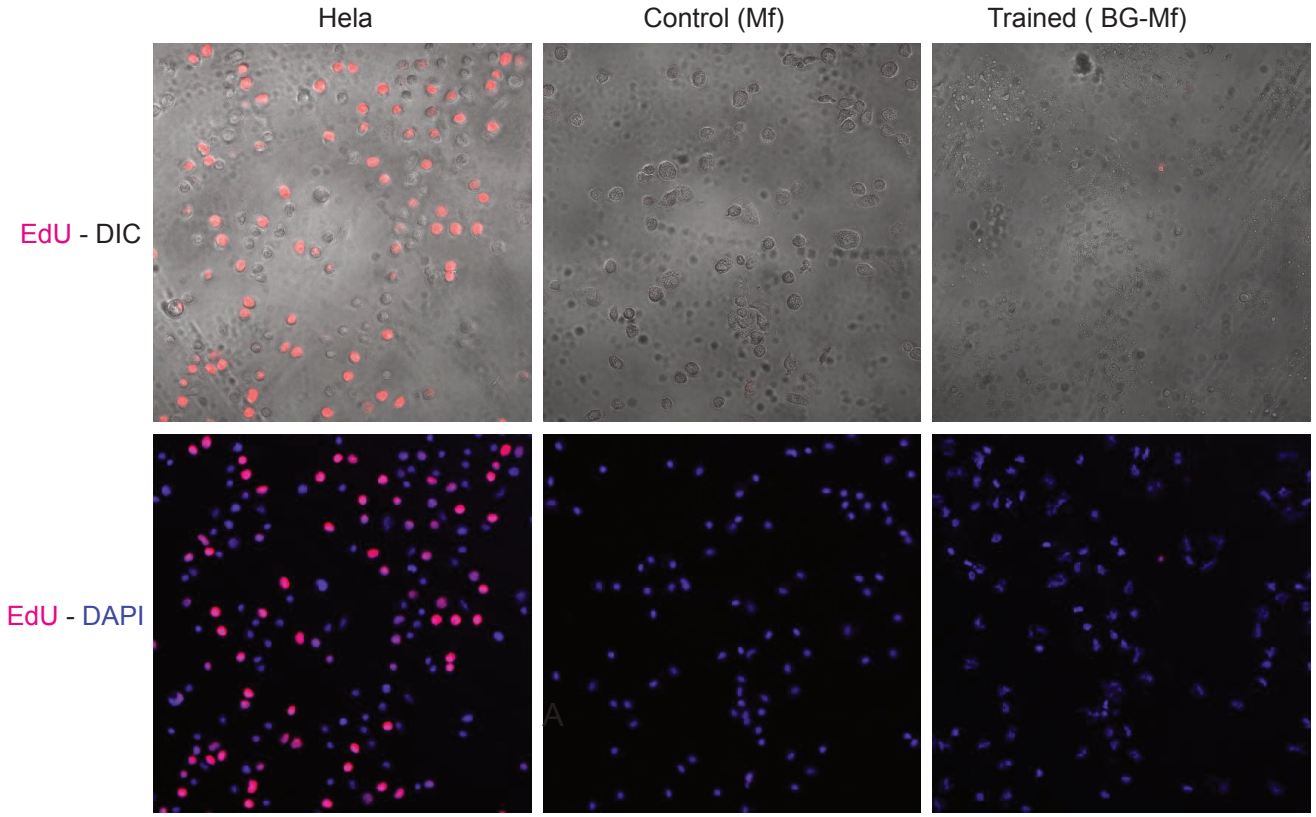

Figure S5

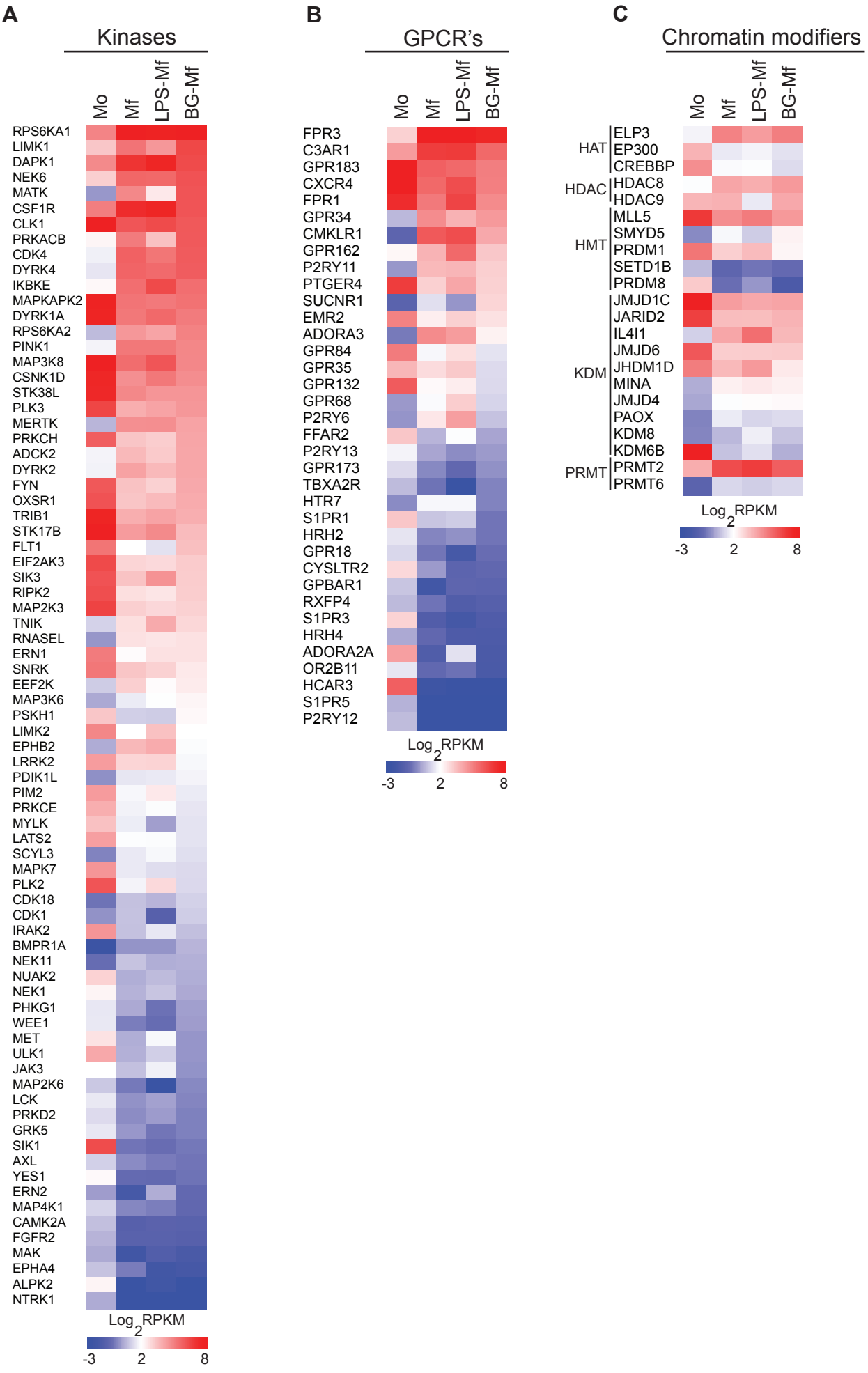
A
Kinases
Mo
Mf
LPS-Mf
BG-Mf
RPS6KA1
LIMK1
DAPK1
NEK6
MATK
CSF1R
CLK1
PRKACB
CDK4
DYRK4
IKBKE
MAPKAPK2
DYRK1A
RPS6KA2
PINK1
MAP3K8
CSNK1D
STK38L
PLK3
MERTK
PRKCH
ADCK2
DYRK2
FYN
OXSR1
TRIB1
STK17B
FLT1
EIF2AK3
SIK3
RIPK2
MAP2K3
TNIK
RNASEL
ERN1
SNRK
EEF2K
MAP3K6
PSKH1
LIMK2
EPHB2
LRRK2
PDIK1L
PIM2
PRKCE
MYLK
LATS2
SCYL3
MAPK7
PLK2
CDK18
CDK1
IRAK2
BMPR1A
NEK11
NUAK2
NEK1
PHKG1
WEE1
MET
ULK1
JAK3
MAP2K6
LCK
PRKD2
GRK5
SIK1
AXL
YES1
ERN2
MAP4K1
CAMK2A
FGFR2
MAK
EPHA4
ALPK2
NTRK1
Log2RPKM
-3
2
8
B
GPCR's
Mo
Mf
LPS-Mf
BG-Mf
FPR3
C3AR1
GPR183
CXCR4
FPR1
GPR34
CMKLR1
GPR162
P2RY11
PTGER4
SUCNR1
EMR2
ADORA3
GPR84
GPR35
GPR132
GPR68
P2RY6
FFAR2
P2RY13
GPR173
TBXA2R
HTR7
S1PR1
HRH2
GPR18
CYSLTR2
GPBAR1
RXFP4
S1PR3
HRH4
ADORA2A
OR2B11
HCAR3
S1PR5
P2RY12
Log2RPKM
-3
2
8
C
Chromatin modifiers
Mo
Mf
LPS-Mf
BG-Mf
HAT
ELP3
EP300
CREBBP
HDAC
HDAC8
HDAC9
HMT
MLL5
SMYD5
PRDM1
SETD1B
PRDM8
KDM
JMJD1C
JARID2
IL4I1
JMJD6
JHDM1D
MINA
JMJD4
PAOX
KDM8
KDM6B
PRMT
PRMT2
PRMT6
Log2RPKM
-3
2
8

Figure S6

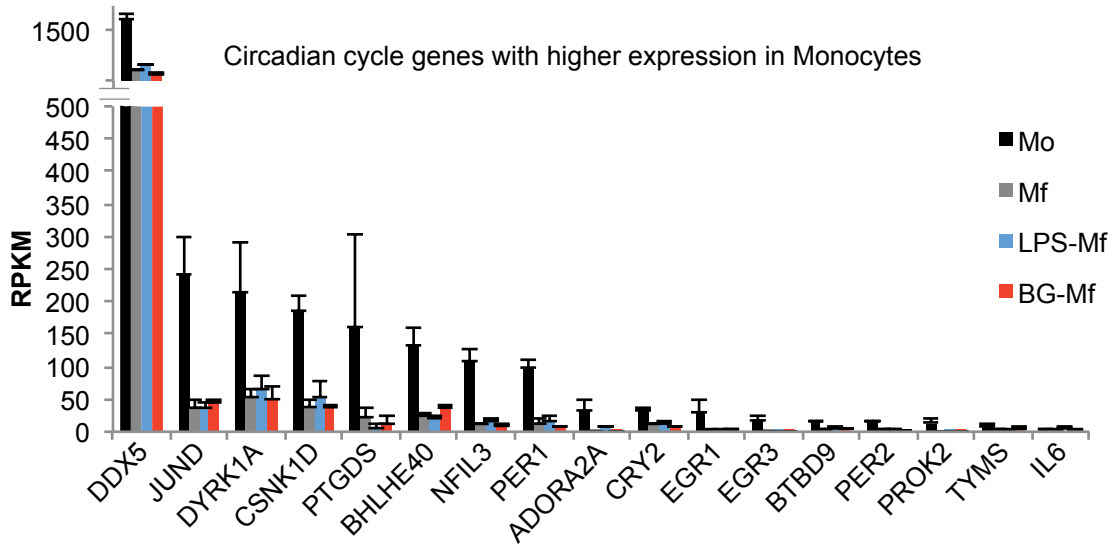

Query:
GO:0007623
GO:0010841
GO:0022410
GO:0032922
GO:0042320
GO:0042321
GO:0042322
GO:0042323
GO:0042745
GO:0042747
GO:0042748
GO:0045187
GO:0045188
GO:0045475
GO:0045938
GO:0046005
GO:0046010
GO:0048512
GO:0060086
GO:0097167

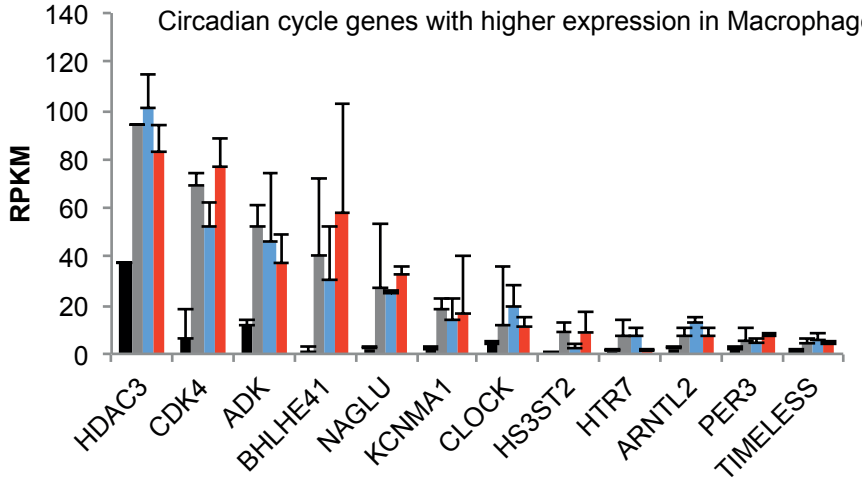

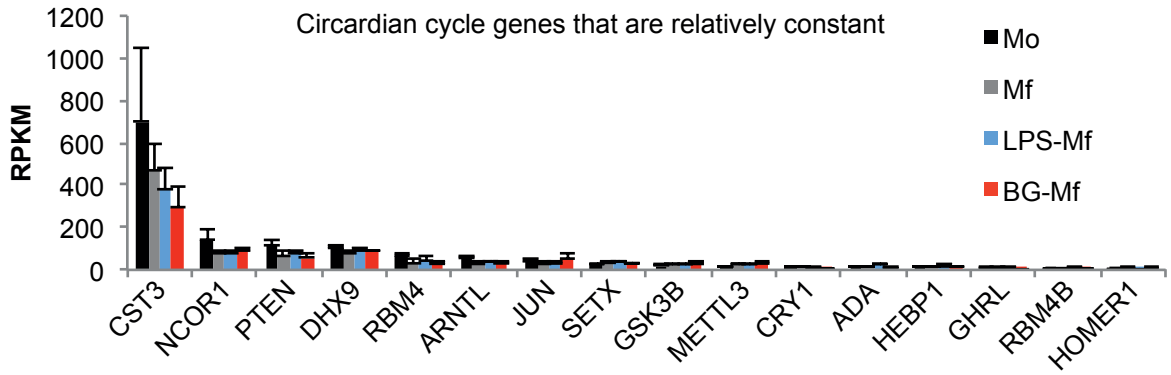

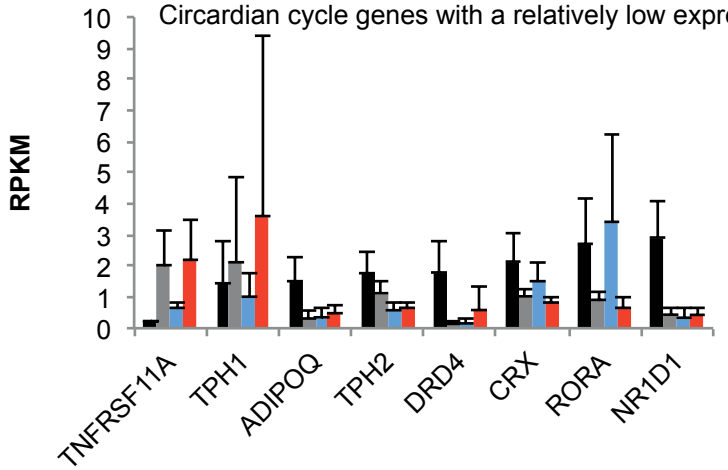

Figure S7

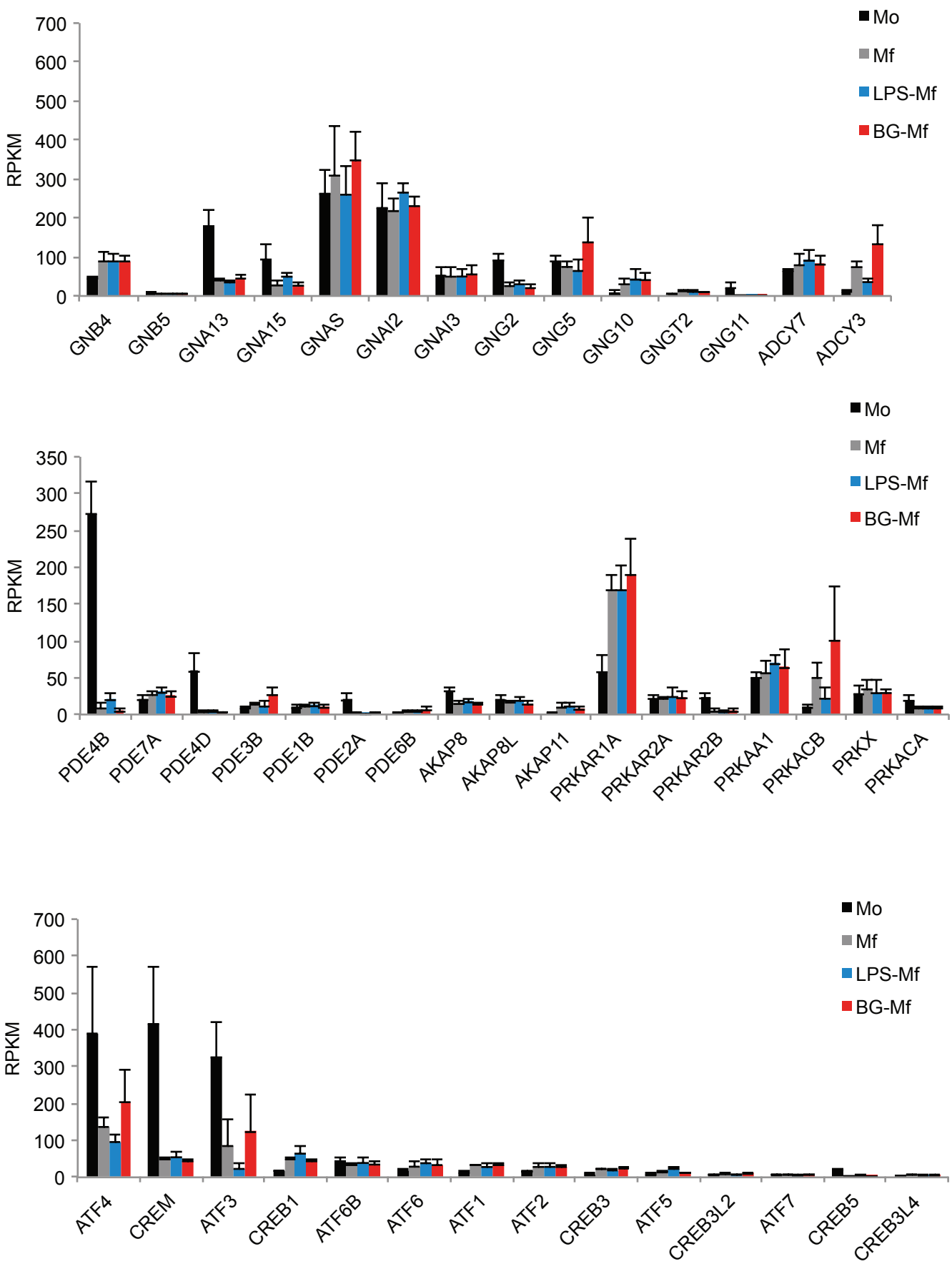
Intracellular cAMP signal transduction molecules
RPKM
Mo
Mf
LPS-Mf
BG-Mf
GNB4
GNB5
GNA13
GNA15
GNAS
GNAI2
GNAI3
GNG2
GNG5
GNG10
GNGT2
GNG11
ADCY7
ADCY3
PDE4B
PDE7A
PDE4D
PDE3B
PDE1B
PDE2A
PDE6B
AKAP8
AKAP8L
AKAP11
PRKAR1A
PRKAR2A
PRKAR2B
PRKAA1
PRKACB
PRKX
PRKACA
ATF4
CREM
ATF3
CREB1
ATF6B
ATF6
ATF1
ATF2
CREB3
ATF5
CREB3L2
ATF7
CREB5
CREB3L4

Figure S8

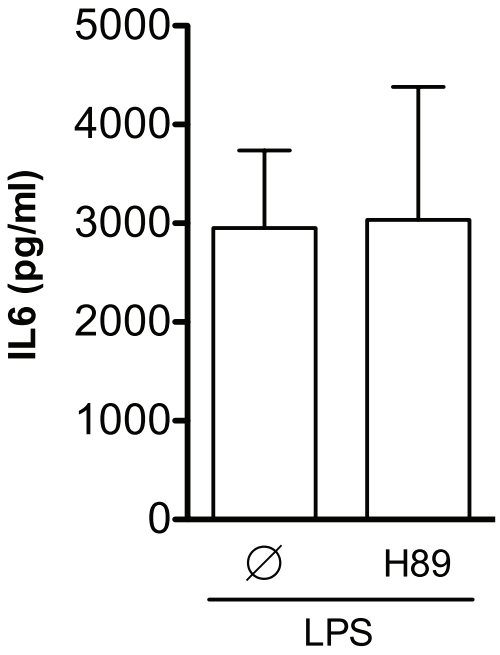
5000
4000
3000
2000
1000
0
IL6 (pg/ml)
∅
H89
LPS

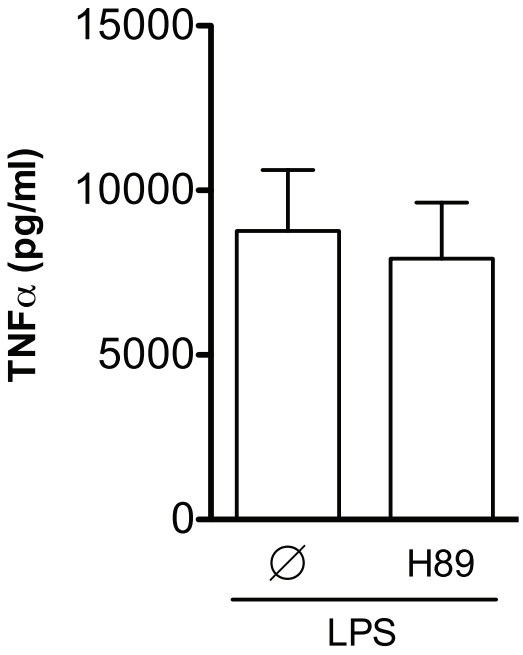
15000
10000
5000
0
TNFα (pg/ml)
∅
H89
LPS

Figure S9